Confinement effects in dendritic growth

1999 J. Phys.: Condens. Matter 11 8981

(http://iopscience.iop.org/0953-8984/11/46/302)

J. Phys.: Condens. Matter **11** (1999) 8981–8993. Printed in the UK PII: S0953-8984(99)05622-2

Confinement effects in dendritic growth

Heike Emmerich†, Detlef Schleussner†, Thomas Ihle‡ and Klaus Kassner†

† Institut für Theoretische Physik, Otto-von-Guericke-Universität, 39016 Magdeburg, Germany
‡ University of Minnesota, Minneapolis, MN, USA

Received 30 June 1999, in final form 27 September 1999

Abstract. We study the interplay between crystal orientation and confinement in diffusion-limited growth. Growth of the overall morphology in the direction of minimal surface stiffness has been investigated in some detail by various authors, the most recent advances being summarized by Brener *et al* (Brener E, Müller-Krumbhaar H and Temkin D 1996 *Phys. Rev.* E **54** 2714). Here, we consider competing influences, each trying to impose a different growth direction. The simplest possible situation giving rise to such a competition is growth in a channel with a mismatch between the orientation of the channel walls and surface tension anisotropy. Analysing this situation, we find a new structure and gain further insight into the problem of morphological stability. Another case is that of periodic boundary conditions, where the same angle of misorientation can be used to describe growth of a *tilted* array of finger-shaped crystals. It is found that the transition between dendritic and doublonic structures is affected by the tilt.

1. Introduction

During the last decade, pattern formation resulting from growth phenomena has attracted increasing interest in many different fields of science [1, 2]. In spite of the vast variety of possible pattern-forming phenomena, people have been able to organize their knowledge in terms of some basic prototypic structures that seem to possess universal properties. Our main interest here lies in diffusion-limited shape evolution, i.e., in structures arising from the transport of a conserved quantity. A canonical example is a crystal growing from its supercooled pure melt, the transported quantity being heat in this case.

In particular, we will assume that the effects of crystalline anisotropy are small enough for facets or missing interface orientations not to occur. For such a system, the stability investigation of simple growth shapes goes back to Mullins and Sekerka [3, 4]. A number of review articles addressing, among other topics, questions of morphology selection have since been published [5–16]. They often focus on problems such as length-scale selection and the 'classical' morphology, the dendrite. Indeed, dendritic patterns are the most frequent microstructures in materials processing. They are known to be solutions of the underlying mathematical problem (described in section 2), if there is a nonvanishing crystal anisotropy, which can be either anisotropy of surface tension or of the coefficient of attachment kinetics.

The limit of vanishing anisotropy remained less clear until recently, when numerical evidence was given for the *doublon*§ as a steady-state solution of this case [17, 18].

At present, doublons are believed to be the building units of the *seaweed* morphology (formerly known under the name of *dense branching* morphology [19]) and there have been

§ *Doublons* consist of two asymmetric fingers of one phase (usually the solid) separated by a narrow channel filled with the second phase (usually the liquid).

0953-8984/99/468981+13$30.00

recent attempts to formulate a theory [20–23] for these fundamental morphologies and the most relevant parameters controlling their appearance. The basic result was a morphology diagram (see figure 1), predicting morphologies as a function of the dimensionless undercooling Δ (the driving force) and the surface stiffness anisotropy ϵ.

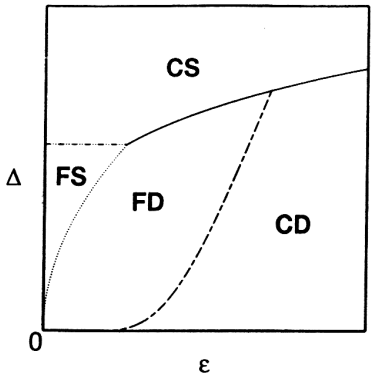

Figure 1. A morphology diagram as given by Brener, Müller-Krumbhaar, and Temkin [23]. The different morphologies are indicated in terms of the controlling parameters Δ (dimensionless undercooling) and ϵ (crystal anisotropy). Altogether we distinguish between compact dendrites (CD), compact seaweed (CS), and the corresponding fractal structures (FD, FS).

The idea of describing experimental observations of certain pattern formation processes in terms of a morphology diagram is now older than a decade [24, 25]. It is based on the concept of nonequilibrium phase transitions, the application of which to morphologies was advocated early on by Ben-Jacob *et al* [26]. However, even for the simplest case of a crystal growing into its undercooled melt with heat being transported by diffusion only, a theoretical foundation for a morphology diagram was given only in 1992 by Brener *et al* [21]. Subsequently, this diagram was refined [23], and one of the suggestions of this article is that further refinement may become necessary in the future.

Besides the distinction between dendrites and seaweeds, referring to the orientational order of the pattern or absence thereof, there is a second classification scheme, concerned with the internal structure of the patterns, namely fractal opposed to compact. Fractals display self-similarity or self-affinity within a range of length scales covering at least one order of magnitude.

In the following, however, we will focus on those parameter regions of the diagram where there is no length scale, below which the evolving structures are fractal, i.e., on the compact morphologies.

In [18], evidence has been given for a first-order transition between the two compact growth morphologies. This problem was also studied in [27–29] within a simplified model, which did not accurately represent the full continuum equations; therefore conclusions about the nature of the transition could not easily be drawn.

A similar transition can be found when studying the system in a narrow channel (figure 2) [30]. Channel growth is interesting, as the idea has been proposed [21, 22] and still lies at the basis of the most recent theory of morphology transitions in diffusion-limited growth [23], that the growth of fingered morphologies might be considered *self-organized growth in channels*. These channels are effectively provided by the neighbours of a particular crystal in the array of dendrites or doublons, and the challenge is the prediction of the array spacing, which is equivalent to the effective channel width.

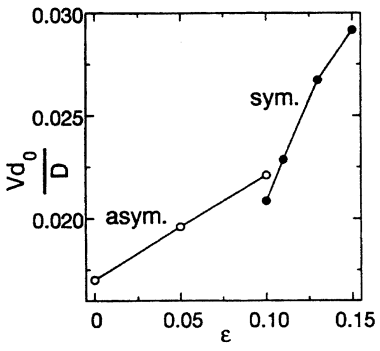

Figure 2. Transition from asymmetric finger solutions to symmetric ones in a narrow channel (the channel width is 200.0 in units of d_0) when the crystal anisotropy ϵ is raised. The solutions are characterized by their nondimensional velocities. This diagram is taken from [30].

In a narrow channel, the dendritic solution corresponds to a symmetric finger, and half of the doublon to an asymmetric one. With that correspondence, the 'narrow-channel' system mirrors the findings in extended systems†. However, it should be noted that there are also differences, and crystal growth in a channel by itself has been intensively studied numerically and analytically; see for example [29–37]. One difference is that whereas dendrites cannot exist for vanishing anisotropy, symmetric fingers can (this is due to the side-walls of the channel providing enough anisotropy). Moreover, the existence domain of symmetric-finger solutions starts off with two branches: one for which the growth velocity decreases with increasing undercooling Δ (and which is irrelevant to dendritic growth) and the other one with increasing velocity, corresponding to the free dendrite in an extended system. Finally, from experience with other systems, such as eutectics [38] and dilute alloys [39], where anomalous cell solutions exist that are akin to doublets of asymmetric fingers, one would expect the transition between symmetric and asymmetric fingers to actually be *supercritical* (see also [40, 41]). Nevertheless, in dynamic simulations, typically a velocity jump is seen (compare figure 2) and symmetric fingers coexist with asymmetric ones, suggesting a *subcritical* bifurcation. A similar situation occurs in the tilt bifurcation of eutectics, where a coupling between the phase of the pattern and the tilt angle renders a supercritical bifurcation effectively subcritical [42, 43]. The bifurcation diagram of steady-state solutions in a channel, including branches of symmetric and asymmetric fingers, has been studied in some detail by Kupferman *et al* [34], and their work seems to resolve the question of coexistence between symmetric and asymmetric fingers in spite of the *supercritical* nature of the basic bifurcation. However, a simple picture as in the case of the tilt bifurcation of eutectics still appears to be lacking.

In this paper, we will concentrate on the correspondence between extended and narrow systems rather than their differences, and proceed as follows. In section 2 we give the mathematical formulation of the situation investigated as well as a brief description of our numerical method. This will be followed by the results for the narrow-channel case in section 3 and those for the system with periodic boundary conditions in section 4. The final section is devoted to a concluding discussion.

2. Mathematical formulation and numerical method

Consider the following situation: a crystal is growing into its undercooled melt, where the growth is controlled by diffusion [9, 44, 45] of the latent heat of freezing. This process

† We consider a channel narrow when its width is less than five diffusion lengths.

is governed by the diffusion equation with appropriate boundary conditions at the moving interface:

$$\partial_t u = D\,\nabla^2 u \tag{1}$$

$$v_n = -D\,\nabla u|_{\text{liquid}}\,\boldsymbol{n} + D'\,\nabla u|_{\text{solid}}\boldsymbol{n} \tag{2}$$

$$u|_{\text{interface}} = \Delta - d(\theta)\kappa. \tag{3}$$

The diffusion field u is the temperature difference referred to the temperature far from the interface and normalized by the ratio of latent heat and heat capacity (which is the temperature increase a solidifying volume element would experience due to latent heat production). D is the thermal diffusivity in the liquid, κ the curvature of the interface.

The physics underlying these equations can be summarized as follows: a solidifying front releases heat which diffuses away as expressed by the diffusion equation. Requiring conservation of energy at the interface results in the Stefan condition (2) for the normal velocity, where the gradients are taken on the liquid and solid sides of the interface, respectively, and D' is the thermal diffusion constant in the solid, usually not much different from that in the liquid. The final equation constitutes the condition of local equilibrium at the interface taking into account the Gibbs–Thomson correction.

For simplicity, we shall only consider the so-called one-sided model [44, 45], i.e., $D' = 0$ (diffusion takes place only in the liquid). This approximation, which is actually unrealistic for thermal diffusion, becomes reasonable in the case of solute diffusion in isothermal solidification. We will use an expression for $d(\theta)$, the anisotropic capillary length, that is slightly different from those used in the literature for fourfold symmetry:

$$d(\theta) = d_0\{1 - \epsilon\cos[4(\theta - \theta_0)]\}. \tag{4}$$

Here d_0 denotes an *average* capillary length† proportional to the isotropic part of the surface energy, ϵ the capillary anisotropy, and θ the angle between the normal to the interface and the overall growth direction that we impose by means of additional boundary conditions (either reflecting walls or periodic boundary conditions). The angle θ_0 describes a mismatch between this overall direction and crystalline anisotropy.

In channel growth, such a mismatch may easily arise, since the original nucleus can have any orientation with respect to the channel walls which confine growth to a given average direction. To state this more precisely: in the centre of the channel, a crystal nucleus will of course start growing along the direction θ_0; however, the wall will prevent it from doing so indefinitely, and once the crystal gets closer to the channel boundary than about one diffusion length, it will feel the modification of the diffusion field due to the presence of the wall, forcing it to change its growth direction. (An isolating wall is impenetrable to the latent heat produced; hence it 'reflects' the latter which heats up the liquid in front of the crystal, impeding further approach to the wall.) As the channel gets filled laterally by the growing morphology, further growth will be possible only in the direction parallel to the walls (i.e., along $\theta = 0$). Hence, the envelope of the morphology will move in this average growth direction. This is the picture for the *average* front between crystal and melt. *Local* features such as tips and branches will still grow along a direction favoured by crystal anisotropy (such as $\theta = \theta_0$ or $\theta = \theta_0 + \pi/2$), *provided* there is enough open space.

On the other hand, if the channel is *narrow* enough, growth may be restricted to a single finger, which will then grow *along* the channel, regardless of the value of θ_0.

For a system with *periodic* boundary conditions, the situation is slightly different. There is nothing to prevent the crystal fingers from growing in the direction surface tension induces

† The average is taken with respect to the angle of orientation θ.

them to choose, given by $\theta = \theta_0$ (since free growth in these systems proceeds in the direction of minimal surface stiffness [44]). However, in this case, the angle $\theta = 0$ corresponds to a direction (the z-axis) which is orthogonal to the periodicity direction (the x-axis). We can, of course, imagine a rotation of the coordinate system leading back to the oft-used expression for $d(\theta)$ with $\theta_0 = 0$. One might then expect that our system would be in no way different from the usual configuration, except that growth occurred along the direction $\theta = \theta_0$ instead of $\theta = 0$. However, such an expectation would be misled. For when rotated back, our system is no longer periodic along the direction given by $\theta = \pi/2$ (the x-axis). To exhibit this on a visual level, we give figure 3, depicting a periodic fingered structure. If we rotated this system anticlockwise by θ_0, then the dashed line would become parallel to the x-axis. Obviously the pattern is not periodic in that direction, due to the finite extension of the fingers in their growth direction, i.e., the presence of tips.

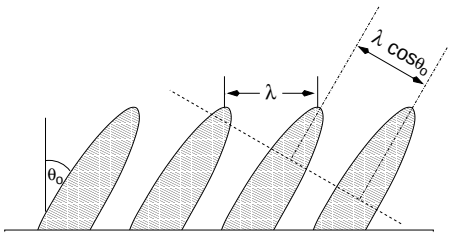

Figure 3. A tilted array of finger-shaped crystals. The array has periodicity length λ along the x-axis. Its spacing in the direction perpendicular to the fingers (dashed line) is reduced by a factor $\cos\theta_0$.

The physics described by (4) with periodicity imposed along the direction given by $\theta = \pi/2$ is that of a *tilted* array of dendrites or fingers. A first description of the latter in the free-growth case has been given by Kupferman and Kessler [40], whereas the more intricate case of directional solidification has been treated in some detail by two groups [41, 46]. For the free-growth case, there is no extensive study yet.

The influence of the tilt angle θ_0 on the pattern will be twofold: (i) the fingers will have to be asymmetric to accommodate the periodicity of the diffusion field in a direction that is not a symmetry direction of the crystal; (ii) the spacing of the tilted array will be shorter by a factor $\cos\theta_0$ than the periodicity length (see figure 3). In saying this, we anticipate that in free growth the crystals will actually grow along the direction θ_0 of minimum surface stiffness (which they would not in directional solidification, due to the influence of the thermal gradient [46], nor in a channel, of course).

The reduction of spacing should, of course, favour slender structures over fat ones, e.g., structures with less side-branching activity are preferred.

So we expect that θ_0 does have an influence on the morphologies arising—obviously due to the periodic images that provide a channel for the crystal. (The angle θ_0 is identical to the angle α_0, defined by Akamatsu and Ihle in their description of similarity laws in the growth of tilted dendritic arrays [46].) We will discuss this in detail in section 4.

Note that tilted arrays are expected to arise in practice: whenever a crystal starting from a single nucleus becomes very large, developing a diamond-shaped envelope [28], the side-branches evolving from the main tips will automatically form a tilted array (see, e.g., figure 3.10 of [15]). In fact, it seems likely that the envelope velocity of large arrays of tilted finger crystals may play an important role in the determination of the average growth velocity of most diffusive growth processes. Hence, a fine tuning of their description beyond that given in [23] would require some knowledge about the behaviour of tilted arrays.

The set of equations (1)–(3) constitutes a *moving boundary* problem, which in essence is a modified *Stefan* [47] problem. Different ways have been sought to deal with such a problem. A most successful approach was based on an integral formulation involving the Green's function of the stationary diffusion equation [48]. Phase-field modelling [49] is a promising approach for future 3D calculations—which however up to now has been restricted to either qualitative computations [50] or small systems [51]—promising, as it allows one to avoid front tracking. In the meantime, we use a finite-difference scheme for solving the diffusion equation. The special feature of our procedure is that of working on several sandwiched grids. The interface is discretized separately, i.e., it does not 'live' on the grid, and it carries along a frame system, to enable treatment of the far system boundaries. At each time step, the full time-dependent diffusion equation is solved on all the grids using boundary conditions on the frame and then calculating the diffusion flux at the moving boundary. To do this, the diffusion field on the frame has to be interpolated from the underlying lattice. Propagation of the interface is done by averaging the interface velocities obtained from the diffusion fields on the different grids. For details of the numerical scheme, refer to [18, 30].

3. The narrow-channel case: periodically oscillating structure

A startling aspect of the doublon is the fact that it consists of two asymmetric fingers. For how can two fingers growing next to one another and *competing* for free space (allowing their latent heat to diffuse away) stabilize each other in a cooperative manner? To some extent this remains a puzzle, as a full stability analysis of the doublon has not yet been performed. A mental picture giving an idea how it can be stable is as follows: if one finger becomes a little faster it will grow ahead and be in a slightly better position for getting rid of its latent heat via diffusion. Thus it will grow thicker. However, the thicker a finger the slower it will continue to grow, due to the fundamental scaling relations connecting growth speed and length scales. Thus its growth velocity will decrease again and the second finger will catch up with it. Now ordinary doublons do not display this behaviour as they are true steady-state solutions of the growth equations. But if they became steady via the stabilization of oscillations of the type described, it is conceivable that under the right conditions it might be possible to observe oscillating doublons. Up to now, these oscillations have remained elusive.

On the other hand, it is known that competing influences on a structure (trying to impose different growth directions) may lead to oscillations†. Therefore it seemed likely that their introduction in the simplest possible manner as realized by our orientational angle θ_0 could be a way to trigger oscillations in diffusive growth systems. Simulating the system with equation (4) for various parameters, we did indeed find a periodically oscillating structure (figure 4).

In what follows, lengths will be given in units of the average capillary length d_0, i.e., the latter is set equal to one and all lengths are given as its multiples. Similarly, time is nondimensionalized by taking d_0^2/D as the time unit. Hence, velocity is measured in units of the thermal diffusivity divided by the average capillary length.

The channel width W is 200 for figure 4, the mismatch angle $\theta_0 = 30^\circ$, the nondimensional undercooling $\Delta = 0.7$, and the surface tension anisotropy is $\epsilon = 0.075$. Evolution of the structure proceeds from the upper left picture to the upper right one and then downwards. That the dynamics of the structure is really periodic can be seen in figure 5, displaying the time evolution of the tip velocity of the large finger on the right-hand side of the channel

† One example where competing influences on dendrites have been studied before is the competition between capillary and kinetic anisotropy [30, 44, 52]. While this may be the most *natural* case to be studied, it is not necessarily the *simplest*, as selection theory would seem to be more complicated than in channel growth with only one type of anisotropy.

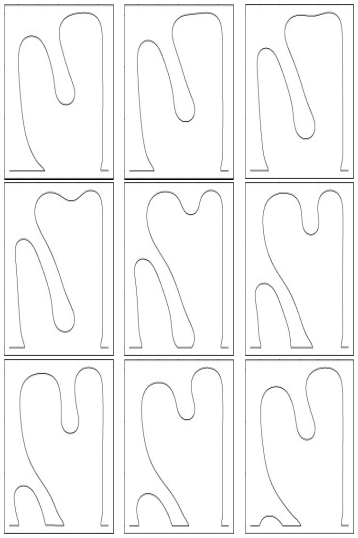

Figure 4. Temporal evolution of the periodically oscillating structure found in narrow channels. Time increases from left to right and from top to bottom. The channel width W is 200.0, $d_0 = 1$, $\theta_0 = 30^\circ$, $\Delta = 0.7$, $D = 1$, and $\epsilon = 0.075$.

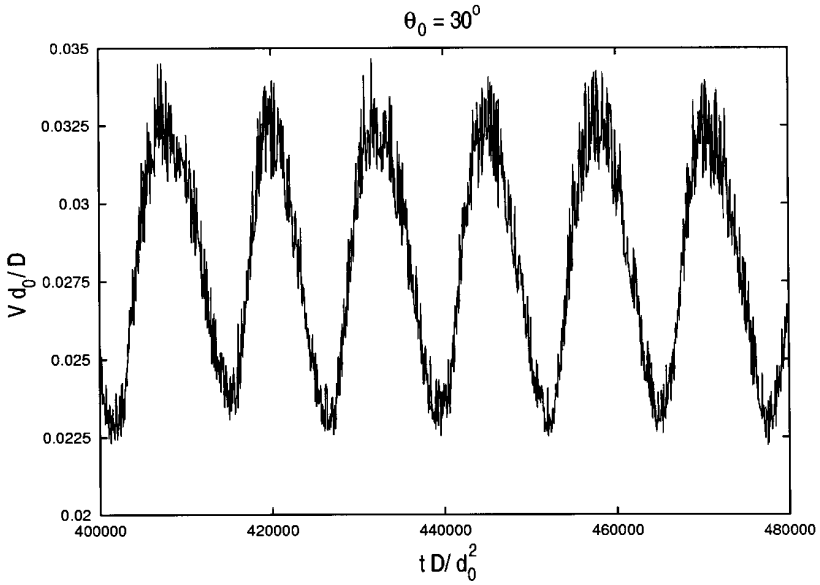

Figure 5. Periodicity of the temporal development of the velocity of the larger finger. For an explanation related to the finger evolution itself, refer to the text.

(figure 4). We clearly recognize a noisy but otherwise sinusoidal oscillation. Fourier analysis of this temporal evolution shows that the amplitude of the basic mode is at least two orders of magnitude larger than that of the next largest mode (suggesting true periodicity, slightly perturbed by numerical noise). This evolution remained stable in simulations for more than 10^5 time units. The periodicity in velocity can easily be understood after a closer look at the

time sequence of figure 4: at first the finger on the right-hand side is quite fat; then it becomes even thicker until it splits off the arm that grows over to the other side of the channel. The thicker the finger the slower it should be. However, in the process of splitting off the second arm, it becomes thinner and increases its speed. Now the second arm on the left-hand side of the channel is thicker and therefore slower. It stays behind and loses the competition for heat diffusion. Finally it dies out on the left-hand side, while the finger on the right-hand side grows thicker again. All that is necessary to avoid chaotic flipping between the left and right fingers (it is always the right one that wins in this example) is that on tip splitting the right finger retains a slight advantage by having a sharper tip. This is essentially guaranteed by its leaning against the right wall.

In a similar way to Brener *et al* [23] when setting up their morphology diagram, we have tried to classify the periodically oscillating structure according to the relevant parameters controlling its appearance. It should be kept in mind, however, that structures appearing in our confined system cannot claim the property of being true phases, first because of the finite lateral size of the system, second because they display an essential dependence on initial conditions. Such a predicate should only be assigned to the *extended* morphologies obtained by the former authors. Nevertheless, dynamic states in small systems *can* shed some light on mechanisms of structure formation, and the periodically oscillating structure may, just like a doublon finger, be considered a building block, playing its role in the evolution of larger structures.

In figure 6, we show the θ_0–ϵ dependence of the structure and its transition to either symmetric or asymmetric finger solutions. During the transition from the asymmetric finger to the symmetric one at the upper left side of the diagram, a velocity jump is known to occur; see

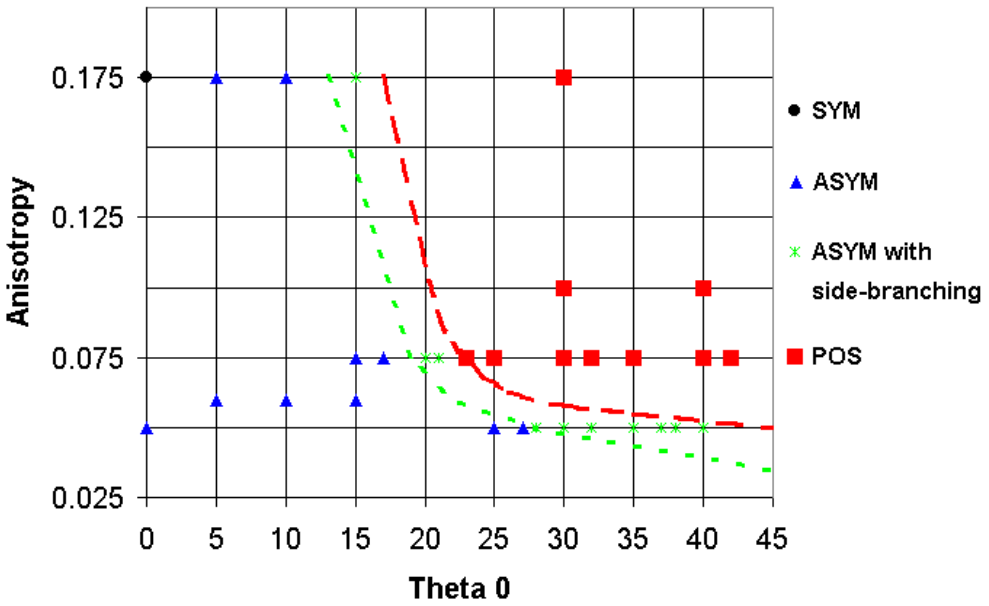

Figure 6. Transitions from symmetric/asymmetric fingers to symmetric fingers with strong side-branching and further to the periodically oscillating structure in the ϵ–θ_0 plane for channel width $W = 200.0$. Our abbreviations should be obvious: SYM, ASYM, and POS refer to symmetric and asymmetric fingers and the periodically oscillating solution, respectively. The undercooling is $\Delta = 0.7$. The dotted lines are conjectured behaviours of the crossover between the different structures. Obviously it is not possible to derive them from single simulations. This calls for an analytical treatment.

figure 2. However, it is known, too, that the velocity of an asymmetric finger does not depend much on the crystal anisotropy [36]; thus following for example the $\epsilon = 0.075$ line from left to right there are hardly any changes in velocity until the regime of periodically oscillating structures is reached. This structure displays velocity oscillations with v-values between $v = 0.0225$ and $v = 0.0345$, where the values stay about constant along the iso-ϵ line.

There is also a dependence of this structure on the channel width W. In the limit of small W, the oscillating solution gets lost in the same way as the asymmetric finger solution for W of the order of 200 and less, and only symmetric fingers can be observed. Extending the system size on the other hand will lead to three-, four-, ... finger solutions with less and less pronounced periodicity in the velocity of one of the fingers. Finally, the structures look just like seaweeds.

The evolution of the periodically oscillating structure seems to be driven by the repeated formation of side-branches. These have a chance to develop due to the main tip being impeded in growth by the wall. As long as the system is not too wide, the wall nevertheless helps the finger leaning against it to survive.

This is related to the mechanism generating the so-called *degenerate morphology* in directional solidification (figure 8.9 in [30]). Another analogy can be seen when comparing the evolution of periodically oscillating structures with the transient of an asymmetric finger (figure 7). The splitting of a second finger growing over to the other side is similar. Therefore, in the terminology of dynamical systems the case of the periodically oscillating structure can be described as a transient becoming a periodic attractor.

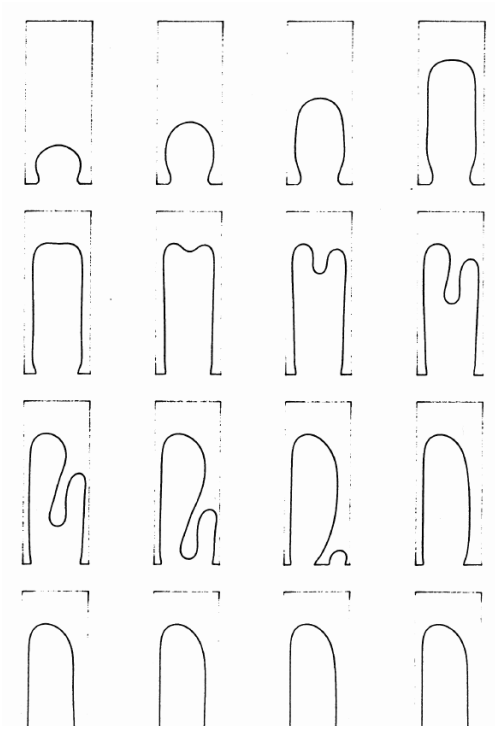

Figure 7. The transient of an asymmetric finger which shows a clear resemblance to the periodically oscillating structure. The evolution is according to [53].

4. Periodic boundary conditions

With periodic boundary conditions, we lose the influence of the channel walls and thereby the competition of growth directions. (This is true as long as there is no external temperature gradient imposing a direction.)

What happens in this case is simply that fingers grow in the direction dictated by surface tension anisotropy (as we neglect kinetic anisotropy). But the structures will not be periodic with respect to the direction orthogonal to this *local* growth direction. Instead we have a tilted array, and we can expect that growth morphologies will show some dependence on the tilt angle in this case.

Figures 8 and 9 are examples of simulated structures. In figure 9, the periodicity length is large enough for a full doublon to develop in the case of lower anisotropy. Both structures are stationary in the usual *statistical* sense, i.e., they grow upward at constant velocity, but their side-branching activity provides them with some additional dynamics, from which we abstract when calling the structure a steady state. (*Rigorous* stationarity would require that there exist a frame of reference in which the structure does not exhibit any movement at all.)

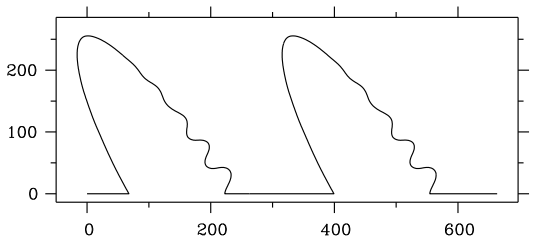

Figure 8. A tilted array of dendrites. Tilt angle $\theta_0 = 30^\circ$, anisotropy parameter $\epsilon = 0.14$, undercooling $\Delta = 0.65$. The periodicity length is 331.6.

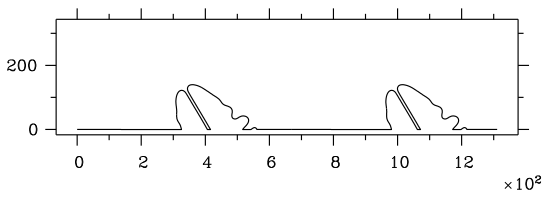

Figure 9. A tilted array of doublons. The periodicity length is 655.3. The anisotropy has been decreased down to 0.1, while the undercooling is larger than in figure 8: $\Delta = 0.8$. Hence, the basic structures that develop spontaneously are doublons, not dendrites.

When the periodicity length becomes very small, we expect single asymmetric fingers to arise (looking roughly like those in figure 3).

Since increasing the tilt angle means decreasing the spacing of the crystal fingers, side-branching will be more strongly suppressed and an array of broken-parity fingers (doubled or not) may be favoured over dendrites. This is borne out by table 1.

Structures created with $\theta_0 = 0^\circ$ were used as initial conditions for the simulations leading to the rotated structures, the velocities of which are given in the right-hand column. That is, we first waited for stationary structures to arise before we 'switched on' the tilt angle θ_0. A rotation by θ_0 moves the transition from dendrites to doublons to lower values of Δ. A glance at the velocities reveals that the rotation slows down the dendritic structures whereas it has little effect on the doublons. This already gives an explanation for the shifted transition, because when several possible stable morphologies compete, it is most of the time the fastest morphology that will win (by occupying the available space) and thus be observed.

The remaining question is that of why the dendrites are slowed down whereas the doublons are not. This is due to the fact that at *given* undercooling, doublons are (if they exist) faster than dendrites; hence their parabolic envelope, still governed approximately by the Ivantsov relation

Table 1. DE denotes dendrites, DO doublons, rDE/rDO the corresponding rotated structures. Dependency of the dendrite–doublon transition on θ_0 and simulated velocities.

	$W = 356.9$	
	$\theta_0 = 0^\circ$	$\theta_0 = 30^\circ$
Δ	v(structure)	v(structure)
0.70	0.048(DE)	0.035(rDE)
0.75	0.067(DE)	0.051(rDE)
0.80	0.103(DE)	0.081(DE) $\rightarrow$ 0.117(rDO)
0.84	0.139(DE)	0.110(DE) $\rightarrow$ 0.169(rDO)
0.85	0.184(DE)	0.184(rDO)
0.86	0.213(DO)	0.213(rDO)

between undercooling and the Péclet number, is slenderer than that of dendrites. Therefore, the latter compete more strongly with their neighbours in the array than the former. Thus dendrites will be slowed down more strongly than doublons. Note that one might expect that for sufficiently large tilt angle the effective channel for a crystal finger to grow along becomes so small that only the symmetric and not the asymmetric fingers could survive. This is not so for two reasons. One is that due to the fourfold anisotropy the maximum tilt angle is 45°. Of course, we could numerically enforce a twofold anisotropy to avoid this. But then the second reason would come into play—the diffusion field is not symmetric about the *local* growth axis in direction θ_0—hence there are no true symmetric fingers, and we have parity breaking (but a trivial variant; the symmetry is broken externally).

The effect of interacting fingers in an array may be regarded as a finite-size effect. Clearly, it should vanish when the distance between neighbouring fingers goes to infinity. We find that the system size does indeed play the expected role (see table 2, where the influence of periodicity is found to be smaller in a system with larger spacing).

Table 2. (Abbreviations as in table 1.) Now the system width is $W = 655.3$. The influence of self-interaction via periodic images decreases with increasing system size (compare with the first table).

	$W = 655.3$	
	$\theta_0 = 0^\circ$	$\theta_0 = 30^\circ$
Δ	v(structure)	v(structure)
0.7	0.048(DE)	0.047(rDE)
0.8	0.103(DE)	0.073(DE) $\rightarrow$ 0.117(rDO)
0.85	0.184(DO)	0.184(rDO)

5. Conclusions

In this paper, we have discussed a periodically oscillating structure found from simulations including a misorientation angle in the angular dependency of the capillarity length. While this structure arises in channels which are probably too narrow to be realized experimentally, it may have some relevance as a building block in extended structures. Oscillatory behaviour may arise in transients of an overall chaotic motion of the pattern. Since it is connected to the side-branching activity of a finger growing in a channel, it may be expected in noisy environments whenever growth can be described by the paradigm of self-organized channel

growth, introduced by Brener, Müller-Krumbhaar, and Temkin [21–23].

In the narrow-channel case proper, we find it important to notice that other stable structures besides the symmetric and asymmetric finger do exist. Here, the influence of the misorientation can turn the transient of a structure into a periodic attractor. At the moment, we are not aware of other examples for such a situation but it would be interesting to look for them for reasons of comparison.

In extended systems, simulated via periodic boundary conditions, we find that dendrites are more strongly sensitive to the interaction with their periodic images than doublons. Since the point of the transition from one structure to the other is also affected by the tilt angle, we expect a refinement of the phase diagram given in [23] to become necessary eventually. In the simplest possible theory given there, a single transition point is assumed to determine the overall morphology for a given value of one of the system parameters. However, this transition point has been calculated under the assumption of free-growth scaling laws. Because in extended systems there is always an interaction with neighbours and, as argued above, parts of the system will always grow under conditions of tilted growth, the same pattern might contain dendrites in parts of its envelope having one orientation and doublons in parts having another orientation. This would smooth out the transition and allow for a richer variety of morphologies.

Acknowledgments

The authors are grateful to Chaouqi Misbah and Heiner Müller-Krumbhaar for fruitful discussions and helpful comments. This work was supported by DFG grant En 278/2-1 (2) in the framework of the research workers' group 'Interface dynamics in pattern forming processes'. We would also like to thank two unknown referees, requiring us to give a more complete list of references and, more importantly, pointing out a lack of clarity in the presentation of the first version of this article.

References

[1] Jullien R, Kertesz J, Meakin P and Wolf D E (ed) 1993 *Surface Disordering Growth, Roughening and Phase Transitions* (Commack, NY: Nova Science)
[2] Ben Amar M, Pelce P and Tabeling P 1991 *Growth and Form: Nonlinear Aspects (NATO ASI Series B, vol 276)* (New York: Plenum)
[3] Mullins W W and Sekerka R F 1963 *J. Appl. Phys.* **34** 323
[4] Mullins W W and Sekerka R F 1964 *J. Appl. Phys.* **34** 444
[5] Parker R L 1970 *Solid State Physics* vol 25 (New York: Academic) p 151
[6] Sekerka R F 1973 *Crystal Growth: An Introduction* ed P Hartman (Amsterdam: North-Holland) p 403
[7] Delves R T 1974 *Crystal Growth* ed B R Pamplin (Oxford: Pergamon) p 40
[8] Flemings M C 1979 *Solidification Processing* (New York: McGraw-Hill)
[9] Langer J S 1980 *Rev. Mod. Phys.* **52** 1
Langer J S 1987 Lectures in the theory of pattern formation *Chance and Matter* ed J Souletie, J Vannimenus and R Stora (Amsterdam: Elsevier) p 629
[10] Coriell S R, McFadden G B and Sekerka R F 1985 *Annu. Rev. Mater. Sci* **15** 119
[11] Kessler D A, Koplik J and Levine H 1988 *Adv. Phys.* **37** 255
[12] Langer J S 1989 *Science* **243** 1143
[13] Ben-Jacob E and Garik P 1990 *Nature* **343** 523
[14] Ben-Jacob E 1993 *Contemp. Phys.* **34** 247
[15] Kassner K 1996 *Pattern Formation in Diffusion-Limited Crystal Growth* (Singapore: World Scientific)
[16] Kurz W and Fisher D J 1989 *Fundamentals of Solidification* (Zurich: Trans Tech Publications)
[17] Ihle T and Müller-Krumbhaar H 1993 *Phys. Rev. Lett.* **70** 3083
[18] Ihle T and Müller-Krumbhaar H 1993 *Phys. Rev.* E **49** 2972
[19] Ben-Jacob E, Deutscher G, Garik P, Goldenfeld N and Lereah Y 1986 *Phys. Rev. Lett.* **57** 1903

[20] Uwaha M and Saito Y 1989 *Phys. Rev.* A **40** 4716
[21] Brener E, Müller-Krumbhaar H and Temkin D 1992 *Europhys. Lett.* **17** 535
[22] Brener E, Kassner K, Müller-Krumbhaar H and Temkin D 1992 *Int. J. Mod. Phys.* **3** 825
[23] Brener E, Müller-Krumbhaar H and Temkin D 1996 *Phys. Rev.* E **54** 2714
[24] Sawada Y, Dougherty A and Gollub J 1986 *Phys. Rev. Lett.* **56** 1260
[25] Grier D, Ben-Jacob E, Clarke R and Sander L M 1986 *Phys. Rev. Lett.* **56** 1264
[26] Ben-Jacob E, Garik P, Mueller T and Grier D 1988 *Phys. Rev.* A **38** 1370
[27] Shochet O, Kassner K, Ben-Jacob E, Lipson S G and Müller-Krumbhaar H 1992 *Physica* A **181** 136
[28] Shochet O, Kassner K, Ben-Jacob E, Lipson S G and Müller-Krumbhaar H 1992 *Physica* A **187** 87
[29] Shochet O and Ben-Jacob E 1993 *Phys. Rev.* E **48** R4168
[30] Ihle T 1996 *Dissertation* RWTH Aachen
[31] Brener E, Müller-Krumbhaar H, Saito Y and Temkin D 1993 *Phys. Rev.* E **47** 1151
[32] Kessler D A, Koplik J and Levine H 1986 *Phys. Rev.* A **34** 4980
[33] Brener E, Geilikman M B and Temkin D 1988 *Sov. Phys.–JETP* **67** 1002
[34] Kupferman R, Kessler D A and Ben-Jacob E 1995 *Physica* A **213** 451
[35] Ben Amar M and Brener E 1996 *Physica* D **98** 128
[36] Ben Amar M and Brener E 1995 *Phys. Rev. Lett.* **75** 561
[37] Kessler D A, Koplik J and Levine H 1986 *Phys. Rev.* A **33** 3352
[38] Kassner K, Valance A, Misbah C and Temkin D 1993 *Phys. Rev.* E **48** 1091
[39] Kassner K, Misbah C, Müller-Krumbhaar H and Valance A 1994 *Phys. Rev.* E **49** 5477
[40] Kupferman R and Kessler D A 1995 *Phys. Rev.* E **51** R20
[41] Okada T and Saito Y 1996 *Phys. Rev.* E **54** 650
[42] Caroli B, Caroli C and Fauve S 1992 *J. Physique* I **2** 281
[43] Kassner K and Misbah C 1992 *Phys. Rev.* A **45** 7372
[44] Brener E and Mel'nikov V I 1991 *Adv. Phys.* **40** 53
[45] Müller-Krumbhaar H and Kurz W 1991 *Phase Transformation in Materials* ed R W Cahn, P Haasen and E J Kramer (Weinheim: VCH)
[46] Akamatsu S and Ihle T 1997 *Phys. Rev.* E **56** 4479
[47] Rubinstein L I 1971 *The Stefan Problem* (Providence, RI: American Mathematical Society)
[48] Saito Y, Goldbeck-Wood G and Mueller-Krumbhaar H 1987 *Phys. Rev. Lett.* **58** 1541
[49] Caginalp G 1989 *Phys. Rev.* A **39** 5887
[50] Kobayashi R 1993 *Physica* D **63** 410
[51] Karma A and Rappel W-J 1996 *Phys. Rev.* E **53** 3017
[52] Ben-Jacob E, Godbey R, Goldenfeld N, Koplik J, Levine H, Müller T and Sander L M 1985 *Phys. Rev. Lett.* **55** 1315
[53] Ihle T 1992 *Diploma Thesis* Leipzig Universiy